





RESEARCH ARTICLE

Scanning macro x-ray fluorescence spectroscopy maps for matching 17th century paintings color areas to different earth pigments uses and for investigating attribution issues

Marco Colombo¹  | Falk Münch¹  | Peter Hoffmann[†]  | Jochen Sander^{2,3} | Wolfgang Ensinger¹ 

¹Department of Materials and Geosciences, Institute of Materials Science, Technical University of Darmstadt, Darmstadt, Germany

²Department of German, Dutch and Flemish Paintings before 1800, Städel Museum, Frankfurt am Main, Germany

³Goethe University Frankfurt, Frankfurt am Main, Germany

Correspondence

Marco Colombo, Department of Materials and Geosciences, Institute of Materials Science, Technical University of Darmstadt, Peter-Grünberg-Str. 2, 64287 Darmstadt, Germany.
Email: colombo@ma.tu-darmstadt.de

Present address

Falk Münch, Materials Chemistry Division, MagnoTherm Solutions GmbH, Darmstadt, Germany.

Funding information

Dr Rolf M. Schwiete Foundation

Abstract

Fe and/or Mn-containing yellow ochre, red ochre, and umber earth pigments are omnipresent in 17th century paintings. Less common in the materials used in historical paintings of this period is the Fe and Mn-rich earth pigment sienna. Different uses of historical pigments in one painting by Georg Flegel (1566–1638) and another version of the same painting but of disputed attribution were recently uncovered by means of macro-x-ray fluorescence (MA-XRF) scanning and other non-invasive analytical techniques. In this paper, an approach solely based upon the correlation of Fe and Mn MA-XRF maps with the optical image of the painting is compared to the use of Mn/Fe correlation plots. The identification of clusters within a plot of the Fe counts vs. the Mn counts can aid to infer whether an area with a certain color matches with the use of the earth pigments found in the two paintings and to ultimately shed light on the different usage of these pigments. The analytical thresholds found in the Mn/Fe correlation plots allowed to identify clusters differing in composition, which matched an area of a certain color with the earth pigments used therein. This highlighted the differences and similarities between the two paintings, ultimately ascertaining the lower value of the painting of disputed attribution. The analysis of single-pixel spectra allowed refining the interpretation of specific Mn/Fe correlation plots. The purpose of these data evaluation steps is presented and the limitations of the proposed methodology are also discussed.

KEYWORDS

correlation plots, earth pigment analysis, historical paintings, MA-XRF, single-pixel spectra

[†] The author passed away in December 2022.

1 | INTRODUCTION

x-ray fluorescence (XRF) spectroscopy is a well-established analytical technique, which features a multi-elemental character, non-destructiveness, selectivity, and ease of analysis. This combination makes it particularly suited for the materials characterization of cultural heritage artifacts.¹ The beginning of XRF for paint analysis can be traced back to the 1970s, with a study featuring the non-destructive examinations of wall paintings as well as panel and canvas paintings.² The development of laboratory-based and portable large-area scanning MA-XRF systems more than a decade ago has triggered a revolution.^{3,4} Compared to point-based XRF spectrometers, an MA-XRF instrument scans the surface of an object with an x-ray beam in the millimeter to micrometer range.⁵ It records a full energy dispersive (ED) spectrum at each step, that is, pixel. After the scanning operation, all the acquired spectra are deconvoluted and elemental distribution maps are obtained utilizing sophisticated data analysis software. In contrast to local point measurements, MA-XRF yields element-specific information over the whole painting (or scanned area). Knowledge of the distribution of painting materials that are present both on surface and in sub-surface layers facilitates a more straightforward interpretation. Furthermore, once the measurement is set-up, the MA-XRF instrument operates autonomously.⁶ Therefore, MA-XRF has also been applied to other cultural heritage objects, such as illuminated manuscripts⁷ and heraldic stained-glass panels.⁸ Even real-time elemental imaging of paintings is possible with a novel mobile MA-XRF scanner.⁹ To obtain information about the chemical bonds of the probed atoms (which ED-XRF analysis cannot provide),¹ coupled scanners were developed recently, for example, MA-XRF/XRPD (x-ray powder diffraction)¹⁰ and MA-XRF/reflectance imaging spectroscopy (RIS)/photoluminescence (PL).¹¹

When investigating pigments in historical paintings, the analysis might reasonably be limited to MA-XRF as key pigments used until the end of the 19th century are mainly inorganic.¹² Consequently, a particular MA-XRF elemental map is probably showing the distribution of the pigment(s) associated with it.¹³ This was utilized for example, to assist a conservation treatment of a 15th century panel painting¹⁴; to solve ambiguities of a painting by the Italian Renaissance Master Raphael.¹⁵ However, a more precise and definitive characterization of the pigments calls for the use of MA-XRF in conjunction with other analytical techniques, such as scanning electron microscopy–energy dispersive x-ray (SEM–EDX) spectroscopy and x-ray radiography,¹⁶ optical coherence tomography (OCT),¹⁷ or synchrotron radiation-based micro-XRF (SR μ -XRF) imaging.¹⁸

Specialized data analysis routines serve as aid to both the data treatment evaluation and the interpretation phases.¹⁹ One example is binary correlation plots, that is, bi-plot graphs in which pixels with similar ratio of total intensities for two elemental lines, extracted from the corresponding single-pixel spectra, form clusters. The selection of clusters and marking of the related pixels in an elemental distribution map can highlight correlations, for example, those belonging to different minerals or soil features in SEM–EDX data of soil aggregates.²⁰ It is also possible to group glass panes and—to a certain degree—attribute them to established types of historical glass²¹ or even to confirm the presence of historical smalt on an oil on panel painting.²² Notwithstanding, the systematic application of correlation plots from MA-XRF data to synthesize those ideas as well as to solve specific research questions, has received less attention. A further important step in MA-XRF image post-processing is the selection of average spectra and single-pixel spectra,²³ that is, each pixel position on the x - y axes and its associated EDX spectrum, from the hyperspectral data cube.²⁰ While average spectra are often reported, for example, to investigate multiple pictorial elements or color zones in a scan²⁴ or to differentiate restored areas from original ones,²⁵ single-pixel spectra have found less space in literature.²⁶ However, the inspection of spectra from single pixels could be useful to solve a specific analytical question related to a particular area of the sample, as the intensity detected at a pixel for a specific sample constituent is representative of the material composition at that x - y location.^{27,28}

Among the pigments found in 17th century historical paintings, the earth pigments yellow ochre, red ochre, and umber are the most common. To a lesser extent, the earth pigment sienna was included in the palette of the masters of that period. The term “sienna” was introduced in Italian and English sources only in the 18th century. As a matter of fact, the name “sienna” is from the Italian area where the pigment was produced, starting from the 18th century.²⁹ However, a yellowish-brown pigment containing iron oxide and manganese oxide was already used before the 18th century. The exact chemistry of siennas has rarely been determined.³⁰ Yellow ochre, red ochre, and umber are iron oxide-rich pigments that contain different amounts of manganese oxide and a large variety of further minerals (e.g., quartz, clays, gypsum, micas, feldspars, etc.) and organic components. Table 1 reports a list compiled from references Eastaugh et al.; Genestar and Pons; and Bikiaris et al.^{30–32} with the main associated color, the minerals, and the Fe and Mn contents of yellow ochre, red ochre, umber, and sienna. The four pigments are associated with different colors and possess different amounts of Fe and Mn. Furthermore, earth pigments can present a range of valid compositions, depending on their purity, origin, and processing. Hence, the elucidation of differences between

TABLE 1 A digest of the information given on the four listed pigments in Eastaugh et al.; Genestar and Pons; and Bikiaris.^{30–32}

Pigment	Main associated color	Mineral(s)	Fe content	Mn content
Yellow ochre	Bright yellow	Goethite (α -FeOOH)	More than 30%	Minor to null
Red ochre	Bright red	Hematite (α -Fe ₂ O ₃)	Up to 70%	Minor to null
Umber	Brown; rich warm brown	Mainly manganite MnO(OH) and pyrolusite MnO ₂	45%–70%	5%–20%
Sienna	Yellow-brown	Mainly goethite (α -FeOOH)	30%–70%	5%–10%

FIGURE 1 (a) Optical image of Inv. 1816; (b) Fe-K α line elemental distribution; (c) Mn-K α line elemental distribution; (d) superposed Fe-K α line and Mn-K α line elemental images, with the Fe and Mn distributions false colored in yellow and red, respectively. The roman numbers from I to IV indicate the locations of the single pixel-spectra extracted from specific areas (see text). [Colour figure can be viewed at wileyonlinelibrary.com]



iron-based earth pigments is a subject of great interest and of ongoing research. In this regard, works have been done by XRF as well as by other means.^{29,31,33–36}

Recently, the 17th century painting “*Still Life with Pike’s Head*” by Georg Flegel (1566–1638) belonging to the Städel Museum’s Old Masters collection and a privately-owned version of the same painting have undergone art historical and art technological studies.^{37,38} In the course of the latter, the yellow ochre, red ochre, and umber earth pigments were found analytically in the two paintings, and the earth pigment sienna might have been used in some areas of both artworks (Städel Museum, Internal Report, 2020). Furthermore, the usage of yellow ochre, red ochre, and umber pigments in the two paintings was found to be different and multifaceted.^{37,38} Another point of interest concerns the general difficulties of chronology and attribution of Georg Flegel’s artworks. In fact, the artist started dating his paintings only in the last years of his artistic career and life.^{37,38} Starting from these bases, the present research aims at maximizing the analytical value of the Fe and Mn MA-XRF maps to infer whether an area with certain colors in the optical images

of the two paintings matches with the use of the diverse earth pigments reported in them. To this end, the Mn/Fe correlation plots of the two paintings are applied systematically and their results are compared to an approach that relies solely on a comparison of the Fe and Mn elemental distribution images with the optical images of the paintings. Additionally, single-pixel spectra selected from specific parts of the datasets are also employed. The second aim of this work is to shed light on the differences in the use of earth pigments in the two paintings.

2 | MATERIALS AND METHODS

2.1 | Paintings

The first painting, “*Still life with Pike’s Head*” (Georg Flegel, c. 1600–10, Inv. No. 1816, oil on oak panel, 31.0 × 40.2 × 0.5 cm), belongs to the collection of the Städel Museum. The second painting is a privately owned version of “*Still Life with Pike’s Head*” (undated, priv-2, oil on oak panel, 31.2 × 41.5 × 0.7 cm). This painting

cannot be attributed to G. Flegel or his workshop without doubt, and is probably a copy.^{37,38}

From the left-hand side to the right-hand side and from the background to the foreground, the artworks (compare Figure 1a) show a glass of wine, a bread placed on the left-hand side, a cup, and apples and their light reflections on the background plate, with the latter placed on top of a bread located on the right-hand side. The foreground depicts coins, a pike's head and two crayfishes placed on top of the left-hand side foreground plate, a knife, an earthenware jug, and hazelnuts placed on top of the right-hand side foreground plate. All depicted objects are placed on top of a table.

The paintings will be referred to below as "Inv. 1816" and "priv-2," respectively.

2.2 | MA-XRF instrumental details

Both artworks were scanned in their entirety by means of a Bruker M6 Jetstream instrument⁴ equipped with a Rh-target x-ray tube, operated at 50 kV voltage and 600 μ A current. A beam size of 100 μ m was achieved through polycapillary optics. The detector of the M6 Jetstream is a 30-mm² Silicon Drift Detector (SDD) and its pulse throughput was set to 275 kcps for both scans. To assure better comparability of the results, the two still lifes were scanned with the same step size and dwell time, 675 μ m and 75 ms/pixel, respectively. Experimental parameters were chosen following the reasoning in Alfeld et al.⁴

2.3 | Mn/Fe correlation plots

As briefly mentioned in the introduction, in a correlation bi-plot of an MA-XRF imaging dataset, for each pixel, the (net) counts of a detected element are plotted against the (net) counts of another detected element in the (x) and (y) axes of said graph, in order to explore their ratio. By coloring the identified clusters with the brushing approach³⁹ and by projecting the existing correlations on an elemental map, the spatial distribution of the brush-selected clusters can be visualized in false-colors.^{20,21} Even if a pigment was more diluted/concentrated when it had been applied (which affects the absolute elemental content of the components), its elemental ratio remains the same. Furthermore, since Mn and Fe are neighboring elements in the periodic table, their secondary XRF radiations are affected by similar attenuation phenomena, provided that no Cr is present. Indeed, in the case of the Mn/Fe x-ray line intensities, the presence of Cr may lead to wrong interpretations as the Fe- K_{α} line (6.40 keV) is strongly absorbed by Cr, with the degree of attenuation at its maximum at the Cr K-absorption edge (5.98 keV), but the Mn- K_{α} line (5.89 keV) is not absorbed

(or absorbed to a lesser extent) by Cr.⁴⁰ It was verified that Cr does not pose a problem here. Consequently, the Mn/Fe fluorescence ratios can be explored even in the non-ideal conditions of MA-XRF analysis on historical paintings (e.g., because of their heterogeneity caused by the intrinsic complexity of the structure of the color layers). Last but not the least, if the radiation of Mn and the radiation of Fe originate from the same layer, their intensity ratio reflects (together with a correction factor depending on the excitation spectrum and layer thickness) their respective concentration ratio. The composite x-ray spectrum found in fluorescence analysis does not only depend on the mass and chemical composition of the sample but also on the excitation conditions and sample thickness.^{41,42} In this regard, the smaller the thickness of the sample, the more negligible are the absorption effects. Furthermore, absorption happening in the detector windows also affects the relative intensities of the lines.⁴³ Therefore, especially due to the uncertainties related to the thickness determination of layers in historical paintings, the precise quantification of the Fe and Mn contents is difficult to be performed.

In the Mn/Fe correlation plots presented in this article, the group of pixels close to the origin ($x: 0; y: 0$) was not analyzed because it was below the significant threshold. Similar clusters of different paintings are represented by the same color.

2.4 | Data processing

The MA-XRF elemental distribution maps of the two paintings were obtained through the Batch Fitting tool of the open-source software package PyMca⁴³ (version 5.8.1, project page at <https://sourceforge.net/projects/pymca/>). The Fe + Mn superposition maps were created with the Bruker M6 Jetstream proprietary software.⁴ The Datamuncher open-source software package⁴⁴ (version 1.4, project page at <https://sourceforge.net/projects/datamuncher/>) was used to display bi-plot graphs and overlay them with a user-chosen MA-XRF elemental distribution map. The single-pixel spectra were manually selected and extracted in the PyMca ROI imaging tool.⁴⁵

In the MA-XRF distribution images presented along this article, the relative abundance of the respective element scales with the pixel brightness.

3 | RESULTS

3.1 | Inv. 1816

In Figure 1, the optical image of Inv. 1816 is shown, along with its Fe and Mn MA-XRF maps and a superposition of both.

Fe and Mn are largely present throughout the painting, see Figure 1b,c. The bright yellow color present on the apples placed on top of the right-hand side background plate as well as their light reflections on it hint at the use of yellow ochre in these areas (Figure 1a). This is corroborated by the absence of Mn in those areas. Similarly, the bright red color present in those areas suggests that a red ochre was used.

However, if for instance considering the right-hand side bread, the objective differentiation between the bright yellow areas and areas of brownish colors is not efficiently made by means of the optical image/MA-XRF maps approach only (Figure 1a–c). This is because (a) Fe is the main characterizing element of the earth pigments, and hence its XRF signal will always be present, irrespective of a potentially different earth pigment used and (b) Mn is present in the brownish earth pigment(s) used to depict the brownish areas of the bread. Consequently, because the brightness level variations of the pixels in the Mn map are not large, it is difficult to match the bright yellow color areas to the possible use of yellow ochre and the brownish color areas to umber.

The superposed Fe + Mn map in Figure 1d confirms the results. The orange color combined Fe + Mn relative intensities (yellow color-coded Fe + red color-coded Mn) in the depicted bread do not help in differentiating the areas of different colors in the optical image.

In Figure 2, the Mn/Fe correlation bi-plot graph and false-color map of Inv. 1816 are shown. In the bi-plot graph (Figure 2a), five different correlation clusters can be distinguished. The green cluster of pixels has its own correlation line. It represents pixels where Mn is not or barely detectable. The yellow, red, blue, and pink clusters share instead the same correlation line. They have at least a few Mn counts. Hence, a potential analytical threshold is created, which could suggest the use of yellow ochre and red ochre by means of the bi-plot green cluster and of umber by means of the remaining clusters, that is, yellow, red, blue, and pink. As expected from the chemical composition of the earth pigments given in Table 1, there is no Mn without Fe, that is, the latter is present in all of the Mn/Fe bi-plot clusters in Figure 2a.

The green cluster distribution in the false-color map of Figure 2b matches with the bright yellow and bright red Fe-rich/no Mn areas in the apples and their light reflections discussed previously. This further underlines the possible use of yellow ochre and red ochre in those areas. The yellow, red, and blue cluster pixels are present in the yellowish-brownish and brownish parts of the apples and in the space in between them (Figures 1a and 2b), suggesting the use of umber in those areas.

In the right-hand side bread, by means of the blue, red, and pink clusters distributions (Figure 2b), it is now

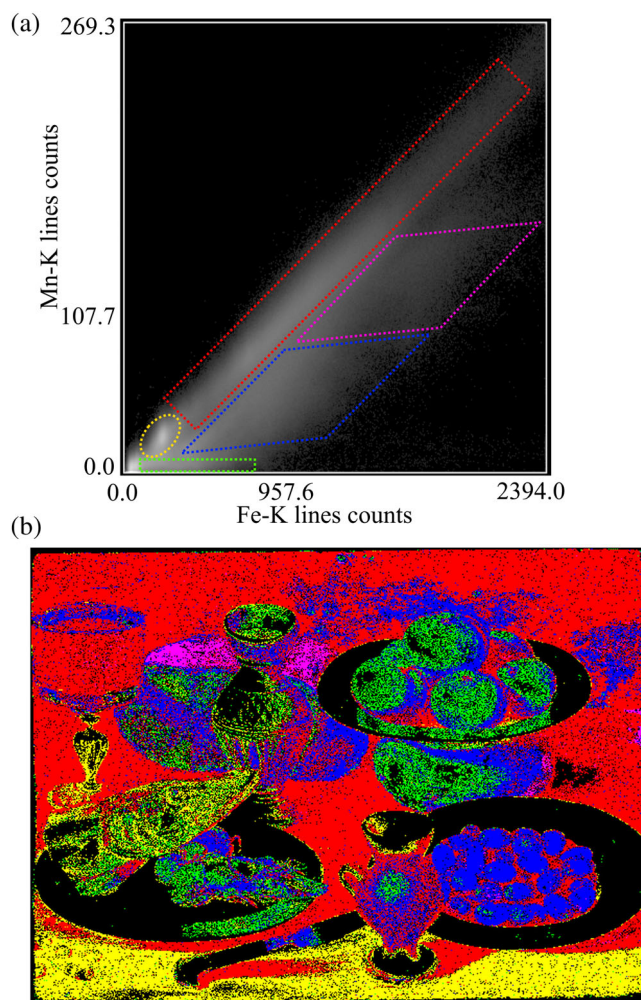


FIGURE 2 (a) Fe-K lines (net) counts versus Mn-K lines (net) counts correlation bi-plot graph of Inv. 1816, with the different colored shapes marking the identified correlation groups; (b) Mn/Fe correlation bi-plot false-color map. [Colour figure can be viewed at wileyonlinelibrary.com]

possible to match the brownish color areas with the possible use of umber. The green cluster distribution in the bread further corroborates the possible usage of yellow ochre in the respective areas with a bright yellow color in the optical image (Figure 1a).

Not all of the green cluster pixels in the false-color map of Figure 2b match with bright yellow and bright red color areas in the optical image. An example is the front side of the left-hand side bread, where the green cluster distribution is mixed with the yellow, red, blue, and pink clusters distributions. Here, as the yellowish-brownish optical color areas on the front of the bread already suggest, umber was possibly used. Despite the non-bright yellow and non-bright red optical colors, the fact that the green cluster pixels are also present in those areas suggests that yellow ochre and/or red ochre might have also been added to the mixture. On top of the bread, in correspondence with the brownish optical areas, only the blue and

pink clusters pixels are present, which again suggests the use of umber (Figures 1a and 2b).

Green, red, and blue clusters pixels match with the hazelnuts in the right-hand side foreground plate, which is in accordance with their brownish color suggesting the possible use of umber (Figures 1a and 2b).

The green, yellow, red, blue, and pink clusters pixels distributions in the foreground earthenware jug matching with brownish optical colors suggest the use of umber (Figures 1a and 2b).

The red cluster pixels distribution in the curvature at the bottom of the handle of the knife agrees with the brown coloration of this depicted detail (Figures 1a and 2b). This again indicates the possible use of umber.

The pixels distributions of the red and yellow clusters in correspondence to the painting background and foreground match well with the gradational earth colors used. The color changes from deep brown in the background toward yellowish-brownish in the table and then to more yellowish in the foreground (the presence of black paint layers in correspondence of the latter is discussed in detail elsewhere³⁸). This corresponds to the red cluster pixels with larger Mn-to-Fe ratio (deep brown and yellowish-brownish colors) and the yellow cluster pixels with high Fe-to-Mn ratio (yellowish color), see Figures 1a and 2b. This highlights the use of umber.

The reader is referred to Table 2 for a full overview of the uses of earth pigments in the different areas of Inv. 1816. In the Inv. 1816 dataset, the element Cr is not present.

3.2 | Priv-2

In Figure 3, the optical image of priv-2 is shown together with the Fe and Mn elemental distribution maps as well as a superposition of the Fe and Mn XRF signals.

The areas with bright yellow and bright red colors that are present in the apples placed on top of the right-hand side background plate as well as in the apples' light reflections on it suggest again the use of yellow ochre and red ochre in these areas (Figure 3a). This assumption is supported by the strong Fe signal in the Fe map of Figure 3b and the concomitant absence of Mn in the Mn map of Figure 3c.

In the right-hand side bread, however, it is again difficult to match the areas of bright yellow color and of brownish-reddish color to yellow ochre and umber, respectively (Figure 3a). The same reasoning regarding the presence of Fe and Mn can be applied as in the case of painting Inv. 1816.

The Fe and Mn superposition elemental distribution map of Figure 3d shows that only the Fe XRF signal

TABLE 2 Different areas of Inv. 1816 and priv-2 and possible uses of earth pigments based on XRF mapping, color from the optical image, and Mn/Fe correlation plots results.

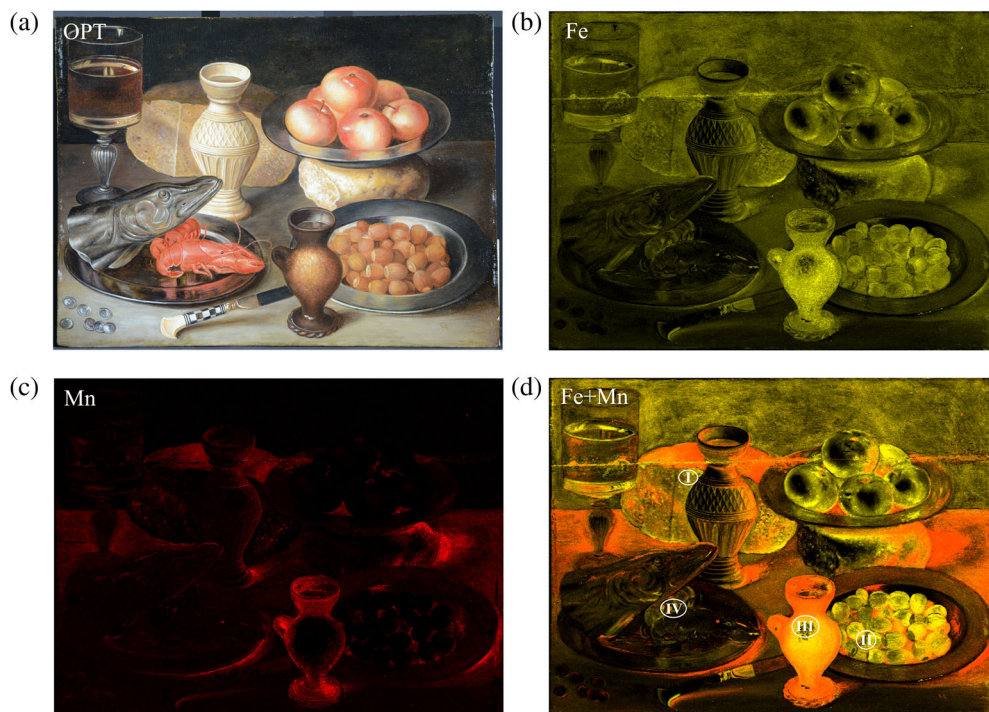
Areas	Earth pigments uses Inv. 1816	Earth pigments uses priv-2
Apples and their light reflections	Yellow Ochre; Red Ochre	Yellow Ochre; Red Ochre
Apples and space in between them	Umber	Umber
Right-hand side bread	Yellow ochre; umber; (red ochre)	Yellow ochre; umber; (red ochre)
Left-hand side bread ^a	Umber; (yellow ochre); (red ochre)	Umber; (yellow ochre); (red ochre)
Background cup	Yellow ochre; umber; (red ochre)	Yellow ochre; umber; (red ochre)
Glass of wine	Umber	Umber; (yellow ochre); (red ochre)
Hazelnuts ^a	Umber; (yellow ochre); (red ochre)	Umber; (yellow ochre); (red ochre)
Hazelnuts light reflections	–	Yellow ochre; (red ochre)
Earthenware jug ^a	Umber; (yellow ochre); (red ochre)	Umber; (yellow ochre); (red ochre)
Knife	Umber; (yellow ochre); (red ochre)	Umber; (yellow ochre); (red ochre)
Knife handle bottom curvature	Umber	Yellow ochre; (red ochre)
Pike's head, crayfishes, light reflections	Red ochre; umber; (yellow ochre)	Red ochre; umber; (yellow ochre)
Background and foreground	Umber	Umber; (yellow ochre); (red ochre)

Note: In the table, an item with two or more pigments is equivalent to the possible use of all of them in the respective areas. Earth pigments listed in brackets are consistent with XRF mapping and Mn/Fe correlation plots analytical results but might only be a minor addition because the color of the area does not coincide with the pigment's main associated color as listed in Table 1.

^aAreas without umber might also contain sienna (see Sections 3.3 and 4).

(color-coded in yellow) is present in the bright yellow and bright red colors areas of the apples and their light reflections (Figure 3a). Next to the Fe signal, the orange color-coded Fe + Mn signal (yellow color-coded + red color-coded) is present in the right-hand side bread.

FIGURE 3 (a) Optical image of priv-2; (b) Fe- K_{α} line elemental distribution; (c) Mn- K_{α} line elemental distribution; (d) superposed Fe- K_{α} line and Mn- K_{α} line elemental images, with the Fe and Mn distributions false colored in yellow and red, respectively. The roman numbers from I to IV indicate the locations of the single pixel-spectra extracted from specific areas (see text). [Colour figure can be viewed at wileyonlinelibrary.com]



In Figure 4, the Mn/Fe correlation bi-plot graph and false-color map of priv-2 are shown. In the bi-plot graph (Figure 4a), three correlation clusters are present. The green cluster of pixels has again its own correlation line, with the Mn signal being not or barely detectable. As before, this cluster likely represents the use of yellow ochre and red ochre. The use of umber is matched with the red and yellow clusters pixels.

An example of the fact that the green cluster pixels in Figure 4b do not always match with bright yellow and bright red colors areas in the optical image of Figure 3a, is again given by the left-hand side bread. The yellow and red clusters pixels distributions on the front of it and on the top of it match with the yellowish-brownish color information in the optical image (Figure 3a). This suggests the use of umber in those areas. Yellow ochre and/or red ochre could also have been added, as per explanation given regarding Inv. 1816. This explanation is also applicable in the following instances where green clusters pixels are found in areas that are correlated with the predominant use of umber.

The green, yellow and, to a lesser extent, red clusters pixels distributions in correspondence of the foreground hazelnuts match with the painted yellowish-brownish-reddish colors (Figures 3a and 4b), pinpointing the use of the earth pigment umber. Strikingly, the bright yellow optical color of the hazelnuts light reflections on the right-hand side foreground plate (Figure 3a) matches with the very high Fe-to-Mn ratio green cluster pixels distribution in these areas (Figure 4b). The match between cluster color and associated optical color (green cluster/bright yellow) suggests that yellow ochre was possibly used.

The brownish-yellowish optical colors of the earthenware jug coincide with the green, yellow, and red clusters pixels distributions (Figures 3a and 4b), which indicates the use of umber.

The bright yellow color in the finely painted curvature of the bottom of the knife handle matches with the green cluster pixels distribution in this specific motif (Figures 3a and 4b). Yellow ochre was possibly used in this area.

Interestingly, the painting background is matched with the green and yellow clusters pixels. The deep-brown color suggests the use of umber. The table with the depicted objects placed on top matches with the yellow and red clusters distributions, indicating that umber was used to achieve those yellowish-brownish-darkish colors areas (Figures 3a and 4b).

For details on the uses of earth pigments in the different areas of priv-2, the reader is referred to Table 2. In priv-2, Cr was used during restoration treatments in areas not affecting the main composition (the priv-2 Cr map is not shown).

3.3 | Single-pixel spectra

In Figures 1d and 3d, the locations from which four single-pixel spectra from the Inv. 1816 and priv-2 MA-XRF datasets were extracted are indicated in the Fe and Mn superposition maps of Inv. 1816 and priv-2. They are localized in the green, yellow, red, and blue clusters pixels distributions of Figures 2b and 4b and correspond in both paintings to the front side of the left-hand side

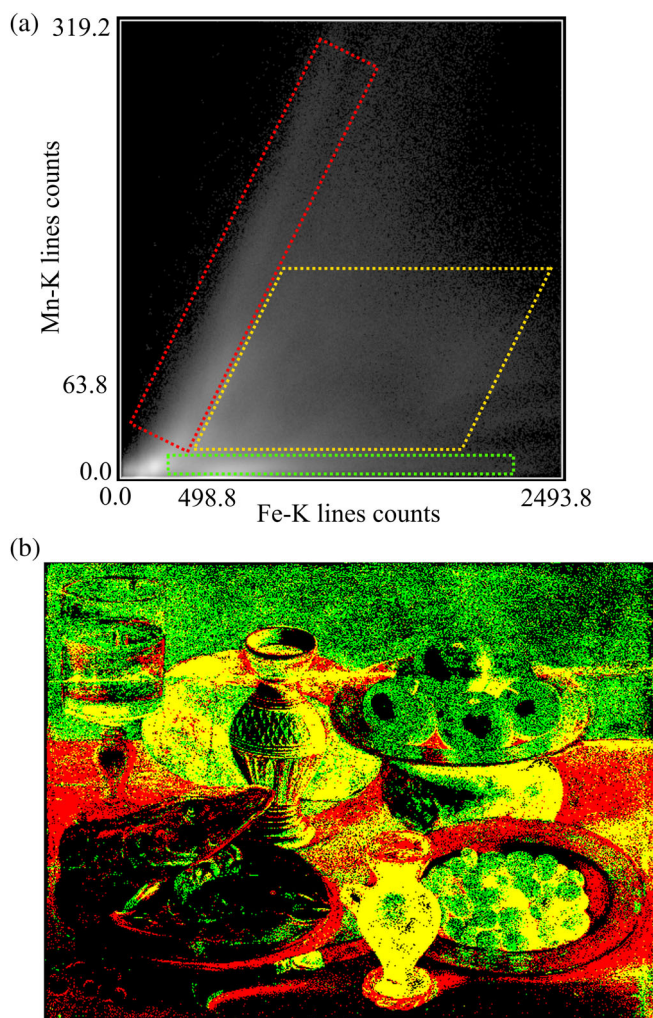


FIGURE 4 (a) Fe-K lines (net) counts versus Mn-K lines (net) counts correlation bi-plot graph of priv-2, with the different colored shapes marking the identified correlation groups; (b) Mn/Fe correlation bi-plot false-color map. [Colour figure can be viewed at wileyonlinelibrary.com]

bread (I), the hazelnuts on top of the right-hand side foreground plate (II), the center of the foreground earthenware jug (III), and the right eye of the left small crayfish (IV).

The spectra of the selected single-pixel in Inv. 1816 and priv-2, labeled (I), (II), and (III), are shown in Figure 5a,b, respectively.

In the optical images (Figures 1a and 3a), the colors from which the single-pixel spectra (I), (II), and (III) were extracted are neither bright yellow nor bright red, as one would expect from the high Fe-to-Mn ratio of the green correlation clusters (Figures 2 and 4). Hence, given the optical image information (yellow-brown color) and the earth pigments found in Inv. 1816 and priv-2 (see Table 1 and Section 1), the earth pigment sienna might have been possibly used in those non-bright yellow and non-bright red colors areas.

As given in Table 1, the pigment sienna has at least a few percent Mn. However, in the single-pixel spectra of Figure 5a,b, in accordance with the green correlation cluster composition, the Mn- K_{α} line does not exceed the noise level. In contrast, the Fe- K_{α} line is clearly visible in Figure 5a,b. This confirms the veracity of the automatic ratio analysis provided by the software, which is found again in the underlying spectra. The difference in signal strength between the Fe- K_{α} lines in Figure 5a,b should be expected based on the green clusters in Figures 2a and 4a. In the Mn/Fe bi-plot graph of priv-2, the green areas reach higher intensities than in Figure 2a. Consequently, spectra extracted from priv-2 MA-XRF dataset will inevitably show higher Fe intensity, which is also confirmed by the presence of the Fe- K_{β} line in Figure 5b in contrast with Figure 5a. Factors such as different layer thickness and presence of other elements might also influence signal strength.

In Figure 5c, the XRF spectra from pure yellow ochre, red ochre, raw sienna, and burnt sienna pigments obtained from the free Pigments Checker v.5© database⁴⁶ are reported. In the respective spectra of raw sienna and burnt sienna, an Mn peak is not present.

The results highlight the difficulties to detect the pigment sienna by means of single-pixel spectra statistics. Furthermore, given the lower order of magnitude of the Fe peaks relative intensities in Figure 5a,b as compared with the same element lines in Figure 5c, a distinction between siennas and ochres, based on the XRF spectra, cannot be performed. However, the latter fact also means that the possibility of the presence of the earth pigment sienna in correspondence to the green cluster areas from which the single-pixel spectra (I), (II), and (III) were extracted cannot be excluded.

The two single-pixel spectra labeled (IV) and selected from Inv. 1816 and priv-2 MA-XRF datasets are shown in Figure 6a,b, respectively.

The areas from which the two single-pixel spectra in Figure 6a,b were extracted (Figures 1d and 3d), match with the brownish optical colors in Figures 1a and 3a. The presence of umber in the areas of the right eye of those small crayfishes is corroborated by the red and blue clusters pixels compositions in the false-color map of Figure 2b and by the yellow and red clusters pixels compositions in the false-color map of Figure 4b.

Both single-pixel spectra (IV) show the presence of the Mn- K_{α} line (Figure 6a,b), which is in accordance with the chemical composition of umber as given in Table 1. The Fe- K_{α} and Fe- K_{β} lines are well-detected, Fe being the main component of the earth pigment umber. Furthermore, despite the XRF spectra shown in Figure 6a,b belonging to different datasets, the order of magnitude of the Fe-K lines is similar. The same holds true for the Mn-K lines.

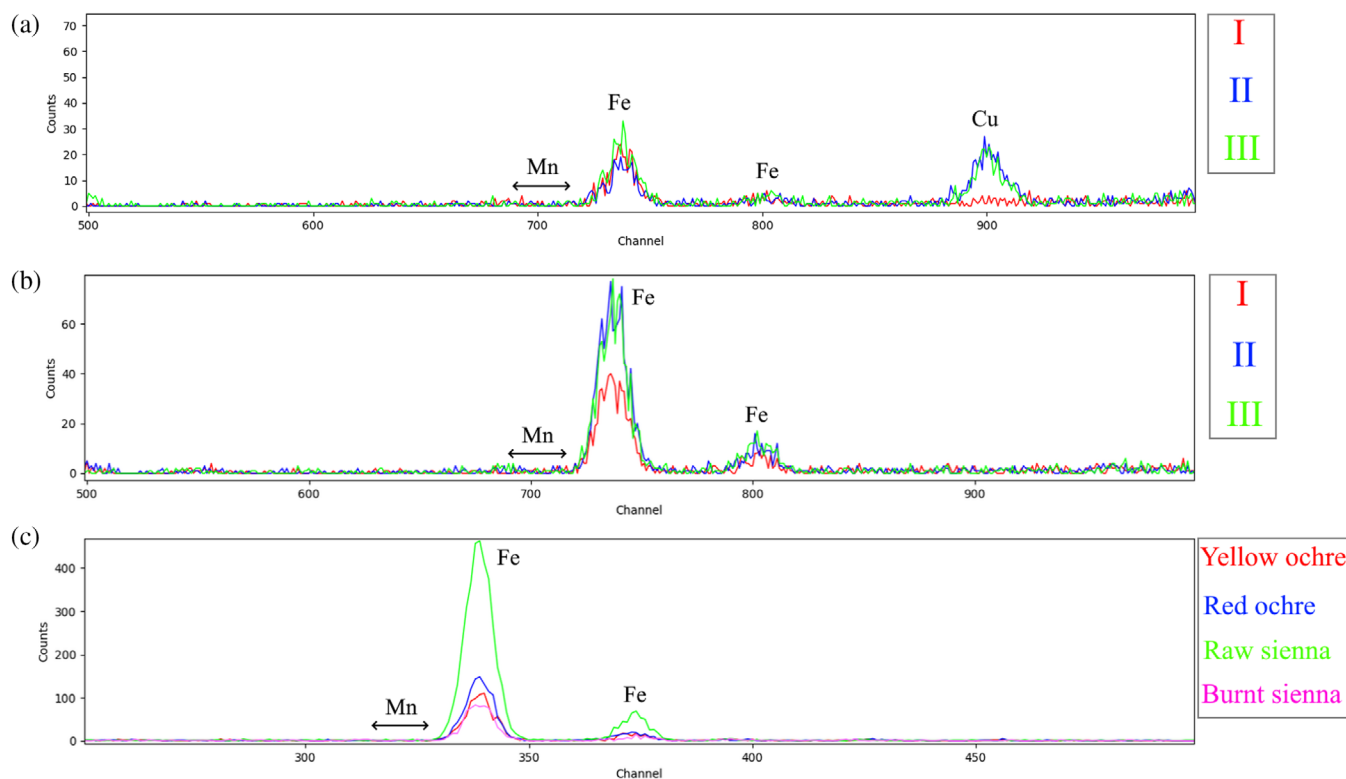


FIGURE 5 (a) Extracted Inv. 1816 single-pixel spectra (I–III); (b) extracted priv-2 single-pixel spectra (I–III); (c) yellow ochre, red ochre, raw sienna, burnt sienna pure pigments XRF spectra database (see text). The misalignment of the x-axis range in (c) in comparison to (a) and (b) reflects the different measurement conditions of the database spectra in comparison to the paintings. [Colour figure can be viewed at wileyonlinelibrary.com]

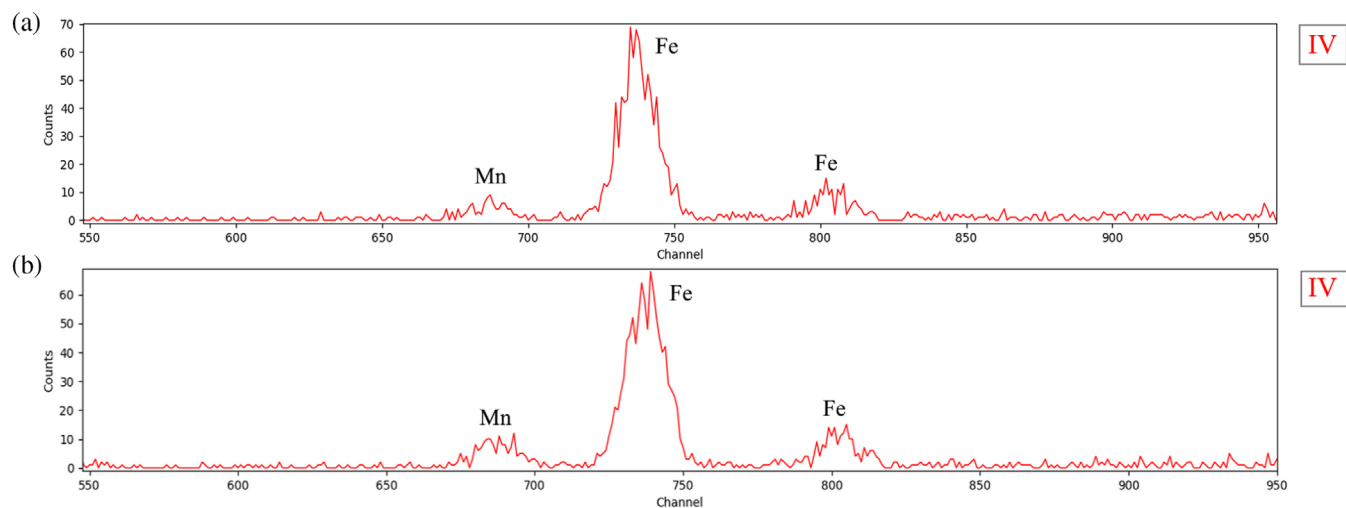


FIGURE 6 (a) Extracted Inv. 1816 single-pixel spectrum (IV); (b) extracted priv-2 single-pixel spectrum (IV). [Colour figure can be viewed at wileyonlinelibrary.com]

4 | DISCUSSION

Table 2 summarizes the different areas and possible associated use of earth pigments across the two paintings based on the results of the XRF maps, optical image color information, and Mn/Fe correlation plots, with the pigments listed in brackets referring to possible minor

additions because of the unmatched color area/pigment's main associated color of Table 1.

Already by means of the paintings optical images/MA-XRF maps approach it was possible to match the areas of the apples, their light reflections, and the space in between the apples in both Inv. 1816 and priv-2 with the possible use of the earth pigments yellow ochre, red

ochre, and umber (Figures 1 and 3). This was feasible because (a) the brown color typical of umber and the bright yellow color typical of yellow ochre are different³² and not adjacent and (b) the pixel brightness is low in the Mn elemental distribution map in areas corresponding of the yellow ochre and red ochre. These earth pigments have only low amounts of Mn, if any (Table 1).

In the right-hand side bread of Inv. 1816 and priv-2 (Figures 1 and 3), the vicinity between the areas of bright yellow color tones and the yellowish-brownish areas prevented the efficient use of the optical images/MA-XRF maps approach to match those areas with the use of yellow ochre and umber pigments. Establishing a meaningful threshold in the Mn map between the presence of pixel brightness, that is, umber, and absence of pixel brightness, that is, yellow ochre, is error-prone. The Fe map is found to be of no help either, Fe being the main characterizing element of earth pigments and hence with a lower variation range than Mn.⁴⁷

Furthermore, by means of the optical images/MA-XRF maps approach, potentially important areas could be overlooked or areas falsely included, for example, because the cutoff threshold in the Mn map was not sufficient to mark a low concentration area or because a suggested Mn area shows a too high or too low Mn/Fe ratio.

In the case of the apples, their light reflections, and the space in between them, the Fe + Mn combination maps (Figures 1d and 3d) could be used as an aid to localize the co-presence of Fe and Mn at a pixel via the orange color-coded Fe + Mn XRF relative intensities distribution (Fe yellow color-coded; Mn red color-coded). However, since the map is the result of the Fe and Mn signals, in the case of the right-hand side bread, it presented the same limitations as the separate Fe and Mn maps discussed above.

The Mn/Fe bi-plot graphs of Figures 2a and 4a allowed to explore the differences between multiple combinations of the two given elements,^{8,21} by assigning to every identified cluster a color and exploring the distribution of the specific cluster pixels composition in order to match different earth pigments uses with their main associated optical color. Specifically, excluding the cluster of pixels close to the origin ($x: 0; y: 0$) an analytical threshold could be defined by means of the correlation group with high Fe counts and low absolute Mn counts close to the origin (green pixels composition in Figures 2a and 4a). For the pixels with more Mn, several correlation groups were chosen (the yellow, red, blue, and pink in Figure 2a and the yellow and red in Figure 4a). The presence of more clusters is advantageous, since different compositions of clusters can match just as many different color tones in the optical image. By manually brush-selecting each correlation group, they were charted in an

elemental distribution image. False-color maps were obtained (Figures 2b and 4b). These colored segmentation maps with the charted clusters allowed matching the cluster pixels compositions with the different color areas in the two paintings. This could locate the uses of yellow ochre and red ochre (green cluster; bright yellow and bright red colors in optical image) and umber (yellow, red, blue, and pink clusters; yellowish-brownish colors in optical image).

Within each cluster, pixels representing a similar composition are found. However, they can match color areas in the paintings that do not match the color expected based on their composition. This is the case with the green cluster pixels in the areas corresponding to the right-hand and left-hand sides breads in Inv. 1816 and priv-2, to the background cups in Inv. 1816 and priv-2, to the glass of wine in priv-2, to the hazelnuts in Inv. 1816 and priv-2, to the hazelnuts light reflections in priv-2, to the earthenware jugs in Inv. 1816 and priv-2, to the knives in Inv. 1816 and priv-2, to the knife handle bottom curvature in priv-2, to the pike's head, crayfishes, light reflections in Inv. 1816 and priv-2, and to the background in priv-2. For these cases, as presented in Section 3 and as given in Table 2, the non-bright yellow and non-bright red colors areas do not exclude the possible uses of yellow ochre and/or red ochre based on the Mn/Fe MA-XRF maps and large Fe-to-Mn ratio green cluster composition. In this regard, the following can be noted:

1. It is not always feasible to correlate a certain composition with a color because the same color can be achieved with different compositions.
2. Pigments of same/similar composition could show different colors.
3. Mixes of pigments are much more difficult to analyze this way.

The latter points highlight the complications caused by the natural compositional range of pigments, which is particularly difficult to resolve if closely related compounds are used, such as in the case of earth pigments. For example, minimal color tones variations can often be the result of natural mixtures that exist with aluminosilicates or smaller proportions of other oxides.³²

Consequently, the optical impression, the chemically expected composition of a pigment, and the spectroscopic information must come together and be interpreted in tandem. Each of these single components is not enough on its own: the color impression can be false, for instance if different pigments with similar color or pigment mixtures are used. The spectral information is not sufficient in cases where the chemical composition of the potentially used pigments is not different enough.

From Table 2, potential differences in earth pigment uses between Inv. 1816 and priv-2 can be inferred. In the glass of wine in Inv. 1816, the presence of the yellow, red, blue, and pink clusters pixels in Figure 2b and the concomitant absence of the typical yellow ochre and red ochre, bright yellow, and bright red colors (Figure 1a) suggest that only umber was used. In the same depicted motif of priv-2, though, the green cluster pixels distribution of Figure 4b suggests that despite the absence of the typical yellow ochre and red ochre, bright yellow, and bright red colors (Figure 3a), these two earth pigments could also have been used next to umber.

Notably, the hazelnuts light reflections were applied with non-Fe and/or Mn-containing pigment(s) in Inv. 1816 (Figure 1b–d), although having a yellowish-brownish color tone (Figure 1a). In contrast, the same light reflections in priv-2 were painted with a Fe-containing earth pigment with barely any Mn (Figure 3b–d). The bright yellow color present in the hazelnuts light reflections in priv-2 (Figure 3a) as well as the co-presence of the green cluster pixels composition (Figure 4b) corroborate the use of yellow ochre in these areas.

Strikingly, the bright yellow color of the curvature present at the bottom of the knife handle in priv-2 matches with high pixels brightness in the Fe elemental map and the concomitant absence of Mn (Figure 3a–d). The presence of the green cluster composition pixels in this painted motif (Figure 4b) confirms that yellow ochre was possibly used here. The fact that a bright red color is absent again does not exclude the possible minor addition of red ochre. However, for the same depicted detail in Inv. 1816, the subtle brownish optical color and the co-presence of Fe and Mn (Figure 1a–c), which is particularly evident with the orange color-coded Fe + Mn XRF relative intensities distribution in the combined map of Figure 1d, suggests that umber was used. The latter is corroborated by the presence of the red cluster pixels distribution in Figure 2b.

Of special note is the comparison of the painting backgrounds of Inv. 1816 and priv-2: in the former, the Städel Museum's still life version, the red and blue clusters pixels representing a large Mn-to-Fe ratio are matched with the brownish-darkish painting background (Figures 1a and 2b). A high Mn amount pinpoints the use of umber as well for achieving these color tones, which is in agreement with the art technological findings in this regard.³⁸ However, the green cluster pixels with a very high Fe-to-Mn ratio match with the brownish-darkish background of the priv-2 painting (Figures 3a and 4b). Only the optical color and the presence, to a much lesser extent than the green pixels, of the yellow

cluster distribution could suggest the use of umber. To achieve the range of shades associated to the latter, a mixing of two earth color grades could have been adopted rather than the application of the pure pigment umber alone, for example, a mixture containing a higher ratio of yellow ochre particles,⁴⁸ which would explain the green cluster large Fe-to-Mn ratio composition distribution in the painting background of priv-2.

After ascertaining the differing art-technology of priv-2 in comparison to Inv. 1816 as well as by taking into account the art-historical view on the painting, the privately-owned version of “*Still Life with Pike's Head*” has been classified to be a contemporary copy, which had neither been painted by G. Flegel nor by his workshop.^{37,38} The abovementioned differences in earth pigments uses between Inv. 1816 and priv-2 in relation to the glasses of wine, the hazelnuts light reflections, and the curvature at the bottom of the knife handle further ascertain the previous findings concerning the disputed attribution of priv-2. Above all, it is the major difference in the use of earth pigments between the painting backgrounds of Inv. 1816 and priv-2 that presents a strong argument for the lower value of the priv-2 still life than the museum version.

The single-pixel spectra extracted from the green cluster-matching areas in correspondence of the front-side of the left-hand side breads, the hazelnuts, and earthenware jugs of Inv. 1816 and priv-2 (Figures 1d, 2b, 3d, 4b, and 5a,b) neither proved the presence of the earth pigment sienna (based on the optical yellow-brown color—Figures 1a and 3a—and the earth pigments found in the two artworks) nor excluded its presence. At least a few percent of Mn should be present in the pigment sienna (Table 1), but Mn is not visible in the single-pixel spectra of Figure 5a,b. The general difficulty in the detection of this pigment via single-pixel spectra statistics was underlined by the XRF spectra of the pure earth pigments raw sienna and burnt sienna obtained from the free Pigments Checker v.5© database⁴⁶ (Figure 5c). As a matter of fact, in these XRF spectra, Mn is not present either. Comparing the different order of magnitudes of the Fe peaks in the single-pixel spectra of Figure 5a,b with those of pure yellow ochre, red ochre, raw sienna, and burnt sienna in Figure 5c has further shown the impossibility to distinguish the earth pigment sienna from yellow and red ochres, based on the XRF spectra. The latter fact means that the possibility of the presence of sienna in the non-umber-rich areas of the left-hand side breads, hazelnuts, and earthenware jugs in Inv. 1816 and priv-2 cannot be excluded (see Table 2).

Single-pixel spectra proved to be useful in order to confirm the presence of Mn in the brown colored and

yellow-red-blue clusters-matching right eye of the small crayfishes in Inv. 1816 and priv-2 (Figures 1a, 2b, 3a, 4b, and 6a,b), ascertaining the use of umber in those tiny areas. As a matter of fact, Mn is the element marker for distinguishing umber.⁴⁸ The similarity between Inv. 1816 and priv-2, given by the presence of umber in correspondence of the tiny detail of the right eye of the small crayfishes, is also highlighted by the same order of magnitudes of the Fe and Mn spectral lines in Figure 6a,b.

The analogy between Inv. 1816 and priv-2 for the depicted right eye of the small crayfishes is consistent with the following facts: priv-2 had probably been painted by a copyist who was not unaware of the painting practices in use in the Flegel's workshop.³⁸ The art-historical view classifies priv-2 to be a copy that was made with great routine achieving Flegel's effects very precisely.³⁷

Single-pixel spectra are capable of recovering information down to the (respective) noise level, although they are characterized by a low number of counts (see Figures 5a,b and 6a,b). This is to be expected for MA-XRF analysis where, due to time constraints, it is often infeasible to set an acquisition time per μm -sized pixel in the order of a second. Hence, single XRF pixel spectra from a MA-XRF scan often suffer from poor signal-to-noise ratio. Average spectra over several pixels possess an improved statistic, and in published research, they are often reported to reveal the presence of element fingerprints corresponding to different materials.^{24,25} However, in the context of the methodology presented here, if taking the tiny detail corresponding to the small crayfishes' right eye in Inv. 1816 and priv-2, from which two separate single-pixel spectra were extracted (Figure 6a,b), it consists of very few pixels (Figures 1–4). In this case, an average spectra selection poses the risk to include pixels from other painted objects as well. Furthermore, averaging the spectra of, for example, 20 adjacent pixels in the painting presents the intrinsic risk to include pixels belonging to different clusters in the bi-plot, that is, the multi-pixel selection is performed via user-chosen elemental distribution maps and not with the false-color Mn/Fe ratio map. For example, if considering the areas from which the single-pixel spectra (I), (II), and (III) in Figure 5a,b were extracted in the false-color maps of Figures 2b and 4b, averaging 20 green cluster pixels spectra is complicated by the presence of the yellow cluster pixels and vice versa. A potential solution would be to employ data analysis routines allowing the average spectra pixels selection within the bi-plot false-color map. To the authors' knowledge, no such routine exists that could handle such big datasets as they are common in MA-XRF.

5 | CONCLUSIONS

We have shown that an approach based on the correlation of Mn and Fe MA-XRF elemental distribution maps and the painting optical image of the painting proved to be valuable to infer whether an area with a certain color matches with the use of yellow ochre and red ochre earth pigments in two 17th century paintings. This is possible because the optical colors of these two historical pigments are different, that is, optically distinguishable, and Mn is present in them only in minor amounts, if any. So, the Mn map can be used to check for the absence of Mn relative intensities in the relevant areas. However, the Mn/Fe maps/optical image approach failed to match color-wise similar areas (e.g., yellow and yellowish-brownish) that are known to be based on different earth pigments, for example, yellow ochre and umber. Thus, the Mn relative intensities are not a safe way to establish whether Mn is still present in a specific area or not. With Fe being the main component of all relevant earth pigments, its elemental map cannot be used for this analytical task either. In this regard, the Mn/Fe correlation plots that were built upon the Mn/Fe total intensities ratio for each pixel and grouped the pixels with similar ratio in clusters were found to be able to match the different cluster compositions with different color areas in the paintings. This highlighted the different uses in earth pigments within the paintings, which ultimately advanced the current understanding of the painting in private ownership providing analytical arguments for its lower value as compared to the museum version. In this regard, it is expected that the methodological approach presented here could be used for more pigments and elemental combinations and could be enlarged to ternary mixtures or more elements (including heavy elements such as Hg and Pb). It could be adapted to the palette of a specific painter for chronology and/or attribution issues related to Georg Flegel or other Old Masters. The systematic application of Mn/Fe correlation plots to answer specific research questions also underlined the limitations of the Mn/Fe correlation plots in specific cases. The latter is especially due to the intrinsic complexity of pigments mixtures used in historical paintings. A comparison between single-pixel spectra, extracted from the same location in the two paintings, and of those spectra with pure earth pigments XRF spectra from a free database, proved the difficulty to detect sienna by means of this spectroscopic data. Furthermore, based on the comparison, it is not possible to distinguish sienna from ochres in those areas in both artworks, that is, the possibility of the presence of sienna cannot be excluded. Single-pixel spectra proved very useful to show the presence of Mn in the same tiny area in the two paintings, revealing the similar

order of magnitudes of the Fe and Mn spectral lines and hence, a similarity in tiny areas. Thus, single-pixel spectra proved to be able to recover information down to the noise level, bringing to light the usefulness of single-pixel spectra statistics for specific analytical tasks. It is expected that a software correlation plot tool that is able to process the large data volume of MA-XRF and allows the selection of average spectra from within each cluster in the colored segmentation map would be helpful to exploit the improved statistic of these spectra for further material characterization challenges.

ACKNOWLEDGMENTS

The authors are indebted to Dr Stefan Flege for the invaluable feedbacks provided during the revision of this manuscript. The authors thank the staff of the Department of Art-Technology and Conservation for Paintings and Modern Sculpture of the Städel Museum for the MA-XRF data acquisition on the two paintings. Ms Brunhilde Thybusch is acknowledged for her technical support during the research project. The authors thank the Dr Rolf M. Schwiete Foundation for financial support. Open Access funding enabled and organized by Projekt DEAL.

DATA AVAILABILITY STATEMENT


The data that support the findings of this study are available from the corresponding author upon reasonable request.

ORCID

Marco Colombo  <https://orcid.org/0000-0002-4471-6380>

Falk Münch  <https://orcid.org/0000-0001-5279-0989>

Peter Hoffmann  <https://orcid.org/0000-0003-0320-1396>

Wolfgang Ensinger  <https://orcid.org/0000-0003-3858-6230>

REFERENCES

- [1] R. Cesareo, G. E. Gigante, A. Castellano, S. Ridolfi, G. Buccolieri, S. A. B. Lins, P. Branchini, in *Advances in Portable X-ray Fluorescence Spectrometry: Instrumentation, Application and Interpretation* (Eds: B. L. Drake, B. L. MacDonald), Royal Society of Chemistry, London **2022**, p. 336.
- [2] R. Cesareo, F. V. Frazzoli, C. Mancini, S. Sciuti, M. Marabelli, P. Mora, P. Rotondi, G. Urbani, *Archaeometry* **1972**, *14*, 65.
- [3] M. Alfeld, K. Janssens, J. Dik, W. de Nolf, G. van der Snickt, *J. Anal. At. Spectrom.* **2011**, *26*, 899.
- [4] M. Alfeld, J. V. Pedroso, M. van Eikema Hommes, G. van der Snickt, G. Tauber, J. Blaas, M. Haschke, K. Erler, J. Dik, K. Janssens, *J. Anal. At. Spectrom.* **2013**, *28*, 760.
- [5] M. Alfeld, *Microsc. Microanal.* **2020**, *26*, 72.
- [6] S. Saverwyns, C. Currie, E. Lamas-Delgado, *Microchem. J.* **2018**, *137*, 139.
- [7] P. Ricciardi, S. Legrand, G. Bertolotti, K. Janssens, *Microchem. J.* **2016**, *124*, 785.
- [8] S. Legrand, G. van der Snickt, S. Cagno, J. Caen, K. Janssens, *J. Cult. Herit.* **2019**, *40*, 163.
- [9] F. P. Romano, C. Caliri, P. Nicotra, S. Di Martino, L. Pappalardo, F. Rizzo, H. C. Santos, *J. Anal. At. Spectrom.* **2017**, *32*, 773.
- [10] F. Vanmeert, N. de Keyser, A. van Loon, L. Klaassen, P. Noble, K. Janssens, *Anal. Chem.* **2019**, *91*, 7153.
- [11] R. Moreau, L. Brunel-Duverger, L. Pichon, B. Moignard, D. Gourier, T. Calligaro, *Eur. Phys. J. Plus* **2023**, *138*, 1.
- [12] A. Impallaria, S. Mazzacane, F. Petrucci, F. Tisato, L. Volpe, *X-Ray Spectrom.* **2020**, *49*, 442.
- [13] F.-P. Hocquet, H. Calvo del Castillo, A. Cervera Xicotencatl, C. Bourgeois, C. Oger, A. Marchal, M. Clar, S. Rakkaa, E. Micha, D. Strivay, *Anal. Bioanal. Chem.* **2011**, *399*, 3109.
- [14] R. Alberti, T. Frizzi, L. Bombelli, M. Girona, N. Aresi, F. Rosi, C. Miliani, G. Tranquilli, F. Talarico, L. Cartechini, *X-Ray Spectrom.* **2017**, *46*, 297.
- [15] C. Ruberto, A. Mazzinghi, M. Massi, L. Castelli, C. Czelusniak, L. Palla, N. Gelli, M. Betuzzi, A. Impallaria, R. Brancaccio, E. Peccenini, M. Raffaelli, *Microchem. J.* **2016**, *126*, 63.
- [16] M. Eveno, E. Ravaud, T. Calligaro, L. Pichon, E. Laval, *Heritage Sci.* **2014**, *2*, 1.
- [17] B. Łydzba-Kopczyńska, M. Iwanicka, M. Kowalska, P. Targowski, *X-Ray Spectrom.* **2021**, *50*, 384.
- [18] G. van der Snickt, H. Dubois, J. Sanyova, S. Legrand, A. Coudray, C. Glaude, M. Postec, P. van Espen, K. Janssens, *Angew. Chem., Int. Ed.* **2017**, *56*, 4797.
- [19] M. Alfeld, S. Pedetti, P. Martinez, P. Walter, *C. R. Physique* **2018**, *19*, 625.
- [20] I. Allegretta, S. Legrand, M. Alfeld, C. E. Gattullo, C. Porfido, M. Spagnuolo, K. Janssens, R. Terzano, *Geoderma* **2022**, *406*, 1.
- [21] S. Cagno, G. van der Snickt, S. Legrand, J. Caen, M. Patin, W. Meulebroeck, Y. Dirckx, M. Hillen, G. Steenackers, A. Rousaki, P. Vandenabeele, K. Janssens, *X-Ray Spectrom.* **2021**, *50*, 293.
- [22] C. Caliri, M. Bicchieri, P. Biocca, F. P. Romano, *X-Ray Spectrom.* **2021**, *50*, 332.
- [23] S. M. Webb, I. McNulty, C. Eyberger, B. Lai, *AIP Conf. Proc.* **2011**, *1365*, 196.
- [24] M. Alfeld, K. Mösl, I. Reiche, *X-Ray Spectrom.* **2021**, *50*, 341.
- [25] H. C. dos Santos, C. Caliri, L. Pappalardo, R. Catalano, A. Orlando, F. Rizzo, F. P. Romano, *Microchem. J.* **2018**, *140*, 96.
- [26] S. Yan, J.-J. Huang, N. Daly, C. Higgitt, P. L. Dragotti, *IEEE Trans. Comput. Imaging* **2021**, *7*, 908.
- [27] D. E. Newbury, D. S. Bright, *Scanning* **2005**, *27*, 15.
- [28] D. S. Bright, D. E. Newbury, *J. Microsc. (Oxford, UK)* **2004**, *216*, 186.
- [29] D. Hradil, T. Grygar, J. Hradilová, P. Bezdička, *Appl. Clay Sci.* **2003**, *22*, 223.
- [30] N. Eastaugh, V. Walsh, T. Chaplin, R. Siddall Eds., *The pigment compendium: a dictionary of historical pigments*, Elsevier Butterworth-Heinemann, United Kingdom **2004**.
- [31] C. Genestar, C. Pons, *Anal. Bioanal. Chem.* **2005**, *382*, 269.
- [32] D. Bikiaris, S. Daniilia, S. Sotiropoulou, O. Katsimbiri, E. Pavlidou, A. P. Moutsatsou, Y. Chryssoulakis, *Spectrochim. Acta, Part A* **2000**, *56*, 3.
- [33] M. Elias, C. Chartier, G. Prévot, H. Garay, C. Vignaud, *Mater. Sci. Eng., B* **2006**, *127*, 70.

- [34] V. Flores-Sasso, G. Pérez, L. Ruiz-Valero, S. Martínez-Ramírez, A. Guerrero, E. Prieto-Vicioso, *Materials* **2021**, *14*, 1.
- [35] R. Lehmann, H.-J. Schmidt, B. F. O. Costa, M. Blumers, A. Sansano, F. Rull, D. Wengerowsky, F. Nürnberger, H. J. Maier, G. Klingelhöfer, F. Renz, *Hyperfine Interact.* **2016**, *237*, 1.
- [36] P. M. Ramos, I. Ruisánchez, K. S. Andrikopoulos, *Talanta* **2008**, *75*, 926.
- [37] A. Pollmer-Schmidt, C. Weber, F. Wolf, *Deutsche Gemälde im Städel Museum 1550–1725*, Deutscher Kunstverlag, Berlin; München **2021**.
- [38] M. Gerken, M. Colombo, A. Pollmer-Schmidt, C. Weber, B. Thybusch, F. Schütt, P. Hoffmann, W. Ensinger, J. Sander, C. Krekel, *Zeitschrift für Kunsttechnologie Und Konservierung* **2021**, *34*, 463.
- [39] G. Sciutto, P. Oliveri, S. Prati, M. Quaranta, S. Bersani, R. Mazzeo, *Anal. Chim. Acta* **2012**, *752*, 30.
- [40] C. Namowicz, K. Trentelman, C. McGlinchey, *Powder Diffr.* **2009**, *24*, 124.
- [41] P. van Espen, F. Adams, *X-Ray Spectrom.* **1976**, *5*, 123.
- [42] R. Sitko, *Spectrochim. Acta, Part B* **2009**, *64*, 1161.
- [43] V. A. Solé, E. Papillon, M. Cotte, P. Walter, J. Susini, *Spectrochim. Acta, Part B* **2007**, *62*, 63.
- [44] M. Alfeld, K. Janssens, *J. Anal. At. Spectrom.* **2015**, *30*, 777.
- [45] M. Cotte, T. Fabris, G. Agostini, D. Motta Meira, L. de Viguerie, V. A. Solé, *Anal. Chem.* **2016**, *88*, 6154.
- [46] R. Larsen, N. Coluzzi, A. Cosentino, *Int. J. Conserv. Sci.* **2016**, *7*, 659.
- [47] D. C. Creagh, D. A. Bradley, *Radiation in Art and Archeometry*, Elsevier Science B.V, Amsterdam, The Netherlands **2000**.
- [48] M. van de Laar, A. Burnstock, *J. Am. Inst. Conserv.* **1997**, *36*, 1.

How to cite this article: M. Colombo, F. Münch, P. Hoffmann, J. Sander, W. Ensinger, *X-Ray Spectrom* **2024**, *53*(2), 139. <https://doi.org/10.1002/xrs.3398>